Deposition Rates from Polydispersed Particle Populations of Arbitrary Spread

For particle deposition from log-normal polydispersed aerosol streams by one or more of several mechanisms described by piecewise-power-law mass transfer coefficients, we derive useful relations between actual total mass deposition rates and the 'reference' rate one would calculate by imagining that all particles in the mainstream population had the average particle volume $\bar{v}(=\phi_p/N_p)$. Included here are diffusion or inertial mechanisms for laminar- or turbulent-boundary layers, free-molecular or continuum diffusion at high Peclet numbers of dense spherical particles, or fractal agglomerates. The mainstream particle volume distribution is considered to be log-normal with arbitrary 'spread' parameter, thereby generalizing earlier results for "coagulation-aged" (self-preserving) distributions. Further generalizations include transitions between important particle transport mechanisms, opening the way to efficient, finite-analytic methods for predicting mass deposition rates for arbitrary, size-dependent particle capture efficiencies.

Daniel E. Rosner
Menelaos Tassopoulos
Yale University
Department of Chemical Engineering
High Temperature Chemical Reaction
Engineering Laboratory
New Haven, CT 06520

Introduction

Background and motivation

It is well known that the ability of an immersed surface to capture particles present in a "dust-laden" mainstream is quite particle-size-dependent, reflecting the mechanism (diffusion, inertia, . . .) of transport (Fuchs, 1964; Friedlander, 1977; Rosner, 1988, 1989). Moreover, in most environments the particle-size distribution (PSD) in the mainstream is itself quite broad, reflecting, of course, the mechanism(s) of particle formation (see, e.g., Flagan and Friedlander, 1978.) Thus, to calculate total mass deposition rates, one must sum (integrate) over both capture efficiency $\eta_{cap}\{v\}$ and the *mass* distribution function $\tilde{\rho}_p\{v\} \cdot v \cdot n\{v\}$, where $n\{v\}dv$ is the particle *number* density between particles of volume v and $v + dv$, with the particle volume treated as a continuous variable (Rosner, 1989).

As in the kinetic theory of gases, it would be useful if the results of greatest engineering interest could be expressed in terms of certain averages characterizing the distribution such as the reference deposition rate, if all particles had the *mean* particle volume: $\bar{v} = \phi_p/N_p$, where ϕ_p is the particle volume fraction (first moment of the distribution). [Recall the utility of such kinetic theory concepts as the *mean* thermal speed (Bernoulli, Maxwell; see, e.g., Garber et al., 1986) and the *mean*-free path (Clausius, Maxwell, and Reynolds).]

$$\phi_p = \int_0^\infty v \cdot n\{v\}dv \equiv \mu_1 \tag{1}$$

and N_p is the total particle number density (zeroth moment):

$$N_p = \int_0^\infty n\{v\}dv \equiv \mu_0 \tag{2}$$

This suggests the following practical approach to estimating total particle mass deposition rates. First, using $\eta_{cap}\{v\}$, one calculates the expected (reference) mass deposition flux $-\dot{m}''_{p,ref}$ if all particles in the mainstream had the same volume $\bar{v}$. Then, one corrects this reference deposition rate by a factor (often quite near unity, see below) which is expected to depend on the "shapes" of the functions $\eta_{cap}\{v\}$ and the PSD $n\{v\}$.

Recent results

For the commonly encountered situation that $\eta_{cap}\{v\}$ or its Stanton number counterpart can be adequately represented by a simple power law and $n\{v\}$ is "self-preserving" (as in "coagula-

tion-aged" aerosols, see, e.g., Friedlander and Wang, 1966; Lai et al., 1977; Friedlander, 1977), we recently presented simple results for $-\dot{m}''_p/(-\dot{m}''_{p,\mathrm{ref}})$ (Rosner, 1989). [Since we frequently must deal with targets that present zero projected (frontal) area, it is more useful to adopt here the dimensionless mass transfer coefficient, St_m, defined by $-\dot{m}''_p/(\rho_p U_\infty)$ (see, e.g., Rosner, 1988).] The results show that the quantities of interest could be obtained directly by merely interpolating previously calculated dimensionless fractional moments of $\psi\{v/\bar{v}\} \equiv n\bar{v}/N_p$ to determine the moment μ_k corresponding to:

$$k = 1 + \left(\frac{\partial \ln St_m}{\partial \ln v}\right) \tag{3}$$

In this way, it was possible to show (Rosner, 1989) that, for say $Pe \gg 1$, convective-diffusion $-\dot{m}''_p/(-\dot{m}''_{p,\mathrm{ref}}) \simeq 0.90 \pm 0.02$ irrespective of turbulence in the boundary layer, particle Knudsen number (Kn_p) and even quasispherical particle morphology (dense vs. fractal agglomerates). [For particle transport in gases, one finds that the Schmidt number $Sc \equiv \nu/D_p$ is quite often so large that large Peclet numbers ($Pe = Re \cdot Sc$) are achieved even when the Reynolds number is *small* (see, e.g., Friedlander, 1977; Fernandez de la Mora and Rosner, 1982).] Particle *inertial* effects were shown to increase $-\dot{m}''_p/(-\dot{m}''_{p,\mathrm{ref}})$ above unity, yielding values near 2.9 for the eddy impaction of $Kn_p \ll 1$ dense spherical particles.

Objectives and outline

It would be valuable to extend these results in two respects. First, we wish to calculate deposition rates from mainstream particle-size distributions which may be much broader or narrower than those pertaining to "coagulation-aged" distributions. Quite often actual aerosol particle populations, generated under a variety of conditions, can be approximated by log-normal distributions (Aitchison and Brown, 1969; Raabe, 1971; Fuchs, 1964 and its references). Furthermore, self-preserving distributions themselves are not very different from log-normals of a specific geometric standard deviation (Lee, 1983; Lee et al., 1984; Ali and Zollars, 1988, for self-preserving distributions due to shear coagulation). Second, we wish to calculate and present useful results for commonly-encountered $St_m\{v\}$ functions that are more complex than a single power law.

This path inevitably leads to a simple, computationally-efficient "finite-analytic" method for calculating total mass deposition rates for the general case of *arbitrary* $St_m\{v\}$ and *arbitrary* PSD $n\{v\}$ by suitably combining our results for "piecewise"-power-law $St_m\{v\}$ functions and log-normal PSD's of arbitrary spread. But perhaps more important than such an "algorithm" is the conceptual content of the results to be presented: i.e., the insight they provide into the factors governing total deposition rates from "polydispersed"-flowing dust-laden fluids. Moreover, we also calculate and present "once-and-for-all" results that enable the rapid estimation of particle mass deposition rates in a rather wide variety of commonly-encountered engineering situations, with the conclusions and implications discussed in the last section.

Table 1. Exponent *b*: Power-Law Dependence of $St_m(v)$ on Particle Volume, v

Sc Exponent	Fractal Dimension (D)*	Knudsen Diffusion	Continuum Diffusion	Eddy Impaction
2/3 (LBL)	3 (dense)	−0.4444	−0.2222	—
2/3 (LBL)	1.8 (aggreg.)	−0.7407	−0.3704	—
0.704 (TBL)	3 (dense)	−0.4693	−0.2347	—
0.704 (TBL)	1.8 (aggreg.)	−0.7822	−0.3911	—
—	3 (dense)	—	—	1.3333

*Here we take $D_p \sim v^{-2/D}$ or $\sim v^{-1/D}$ for free-molecular and continuum diffusion, respectively (Mountain et al., 1986). D is the fractal dimension, equal to 3 for dense particles and equal to about 1.8 for diffusion-limited aggregates (Meakin, 1983).

Deposition from Log-Normal Distributions When $St_m\{v\}$ Is a Power Law

Consider an aerosol with particle-size distribution function, $n\{v\}$, outside the gaseous boundary layer. In terms of the dimensionless mass transfer Stanton number $St_m\{v, \ldots\}$ (Rosner 1988, 1989), the total mass deposition rate is given by:

$$-\dot{m}''_p = U \cdot \int_0^\infty St_m\{v, \ldots\} \cdot \tilde{\rho}_p \cdot v \cdot n\{v\} dv \tag{4}$$

where U is the gas-free stream velocity, and $\tilde{\rho}_p$ is the intrinsic particle density, assumed to be independent of particle size. As already indicated, we will focus attention on the comparison between the total mass deposition rate $-\dot{m}''_p$ and the *reference* deposition rate, $-\dot{m}''_{p,\mathrm{ref}}$, from a hypothetical monodispersed population comprising particles, each having the size (volume) $\bar{v}$; i.e.,

$$-\dot{m}''_{p,\mathrm{ref}} \equiv U \cdot St_m\{\bar{v}\} \cdot \tilde{\rho}_p \cdot \bar{v} N_p \tag{5}$$

If we further denote by R the deposition rate ratio that we seek, then

$$R \equiv \frac{-\dot{m}''_p}{-\dot{m}''_{p,\mathrm{ref}}} = \int_0^\infty \frac{St_m\{v\}}{St_m\{\bar{v}\}} \cdot \frac{v \cdot n\{v\}\, dv}{\bar{v} N_p} \tag{6}$$

As noted earlier (Rosner, 1989), if deposition occurs due to *either* convective Brownian diffusion *or* eddy impaction alone, then we may take $St_m \sim v^b$ throughout the particle volume range of interest; for example, we may assume a power-law form for the dependence of the local mass Stanton number on particle volume, where b is determined by the nature of the deposition mechanism, Knudsen number, and fractal dimension of the particles. In Table 1, we give some typical values for the exponent b for each of the above-mentioned cases. Substituting the power-law form for St_m into Eq. 6, we obtain

$$R = \int_0^\infty \left(\frac{v}{\bar{v}}\right)^{1+b} \cdot \frac{n\{v\}}{N_p} dv \tag{7}$$

From Eq. 7, we see that at least for the case of deposition in a regime over which $St_m\{v\}$ has a single-power-law dependence, in order to obtain R, we simply have to evaluate an appropriate moment $k(=1+b)$ of the mainstream aerosol PSD.

Assuming a log-normal aerosol PSD at the outer edge of the gaseous boundary layer, we may write $n\{v\} = N_p \cdot C_1\{v\}$, with

$C_1\{v\}$ the normalized log-normal particle-size (volume) distribution function defined by

$$C_1\{v\} = \frac{1}{v \ln \sigma_g \sqrt{2\pi}} \exp\left[-\frac{\ln^2\{v/v_g\}}{2 \ln^2 \sigma_g}\right] \quad (0 < v < \infty) \quad (8)$$

where v_g is the median volume of the distribution (or geometric mean) and σ_g is the corresponding geometric standard deviation of the distribution. [The PSD function based on particle radius (here we assume spherical particles), say $C_1\{r\}$, is also log-normal, with median r_g determined through $v_g = (4/3)\pi r_g^3$ and standard deviation equal to $\sigma_g^{1/3}$.] The arithmetic mean of $C_1\{v\}$, written $\bar{v}$ and chosen as our reference particle dimension, is related to the median v_g which appears explicitly in Eq. 8 through (see, e.g., Raabe, 1971):

$$\bar{v} = v_g \exp\{\tfrac{1}{2} \ln^2 \sigma_g\} \quad (9)$$

Combining now Eq. 7, 8 and 9, we find

$$R = \left(\frac{v_g}{\bar{v}}\right)^{1+b} \cdot \int_0^\infty v_*^{1+b} C_1\{v_*\}\, dv_* = \exp\left\{-\frac{1+b}{2} \ln^2 \sigma_g\right\} \cdot \int_0^\infty v_*^{1+b} C_1\{v_*\}\, dv_* \quad (10)$$

where $v_* \equiv v/v_g$ and $C_1\{v_*\}$ is a log-normal distribution with median equal to unity and standard deviation equal to σ_g. Equation 10 can be simplified further, if we note that the kth moment of any log-normal function can be expressed in terms of another log-normal with the same standard deviation and a different median, v_k (Raabe, 1972). Specifically, if we take the original log-normal to be $C_1\{v\}$ as defined in Eq. 5, then one can show that:

$$v^k C_1\{v\} dv = \exp\left[k \ln v_g + \frac{k^2}{2} \ln^2 \sigma_g\right] \cdot \left\{\frac{1}{(v/v_k) \ln \sigma_g \sqrt{2\pi}} \exp\left[-\frac{\ln^2\{v/v_k\}}{2 \ln^2 \sigma_g}\right]\right\} d\left(\frac{v}{v_k}\right) \quad (11)$$

where the new median v_k is determined by:

$$\ln v_k = \ln v_g + k \ln^2 \sigma_g \quad (12)$$

Making use of these relationships and further noting the normalization condition:

$$\int_0^\infty C_1\{v\}\, dv = 1$$

we finally obtain the remarkably simple result:

$$R = \exp\left[\frac{b(1+b)}{2} \cdot \ln^2 \sigma_g\right] \quad (13)$$

Thus, when the mass transfer coefficient $St_m\{v\}$ can be represented by a single power law ($\sim v^b$), Eq. 13 gives the total mass deposition rate compared to the corresponding deposition rate for a hypothetical monodispersed population of particles of individual volume $\bar{v}$, in terms of the actual deposition mechanism (consistent with the choice of b), and the standard deviation (spread) of the depositing aerosol main-stream particle-size distribution.

In Figure 1 we plot the deposition rate ratio R vs. the standard deviation of the aerosol PSD, σ_g, for *continuum* diffusion of dense or fractal particles through laminar (LBL) or turbulent boundary layers (TBL). For the exact "order" $k[(=1+b)$ in Eq. 13] of the corresponding moments, see Table 1. In Figure 1, we also mark the σ_g value at which the log-normal and the self-preserving distributions are approximately the same. [Lee (1983) reports that a log-normal particle-size distribution that is based on *linear* size, such as the particle radius, is similar to the self-preserving distribution for $\sigma_g \simeq 1.32 - 1.35$. We use a PSD based on particle volume, and hence the corresponding standard deviation at which it will become similar to the self-preserving one is for $\sigma_g \simeq 1.35^3 = 2.46$, as mentioned previously.] Note the fair agreement between the self-preserving PSD results of Rosner (1989) for R and our present results for the nearest log-normal PSD.

Figure 2 shows the corresponding total deposition rate ratios R vs. σ_g for Knudsen ($Kn_p \gg 1$) diffusion. It is interesting to note that while in continuum diffusion and for a PSD of arbitrary σ_g, dense particles deposit at higher normalized rates than fractal aggregates, in the free molecular regime the opposite occurs. It is straightforward to explain this behavior if we realize that $R(b)$ (Eq. 13) has a local minimum at $b = \frac{1}{2}$. In the continuum regime as we go from dense to fractal particles, the order of the relevant moment decreases from 0.78 for LBL and dense particles to 0.61 for TBL and fractal aggregates, thus making the corresponding deposition rate ratio decrease too. On the other hand, for Knudsen diffusion, dense particles correspond to moments of order 0.56–0.53 (Table 1), e.g., close to the regime where the minimum of R lies, while fractal particles with

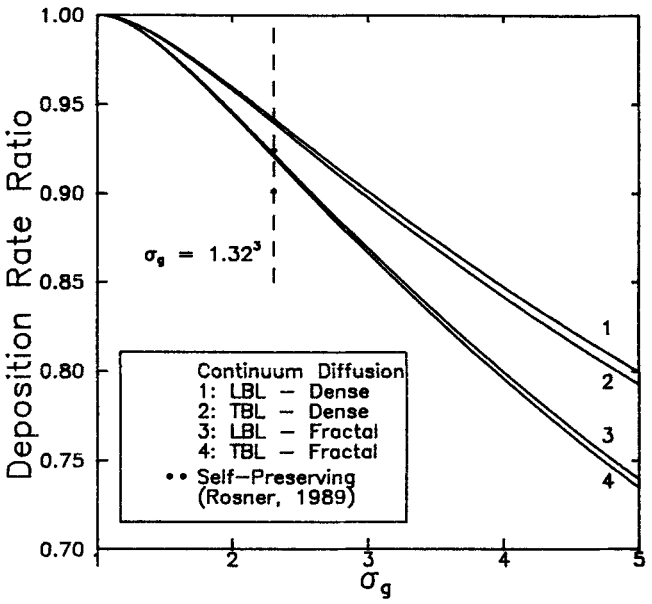

Figure 1. Deposition rate ratio, R, vs. the standard deviation, σ_g, of the aerosol PSD for *continuum* diffusion of dense or fractal particles through laminar or turbulent boundary layers.

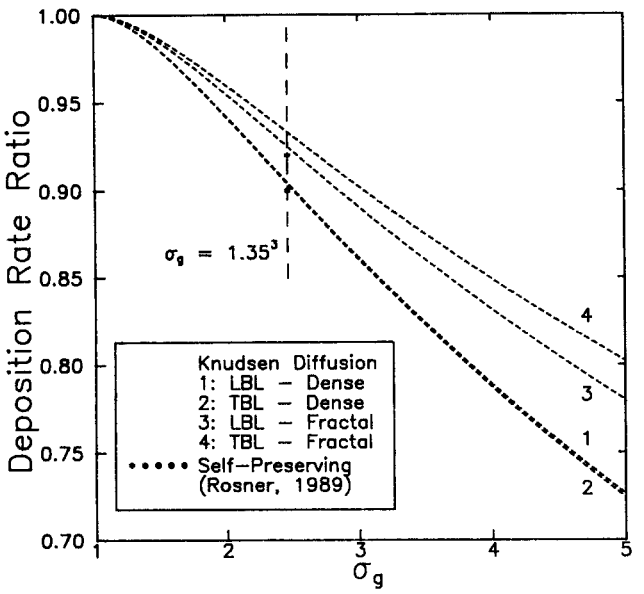

Figure 2. Deposition rate ratio, R, vs. the standard deviation, σ_g, of the aerosol PSD, for *Knudsen* diffusion of dense or fractal particles through laminar or turbulent boundary layers.

required moments in the range of 0.26–0.22 yield higher deposition rate ratios.

In Figure 3 we plot deposition rate ratio against the standard deviation of the log-normal distribution for eddy impaction in the $(t_p^+)^2$ regime (see also Table 1). Since higher σ_g values result in a larger fraction of the total aerosol mass associated with large particles, in this regime the relative deposition rate is an increasing function of σ_g.

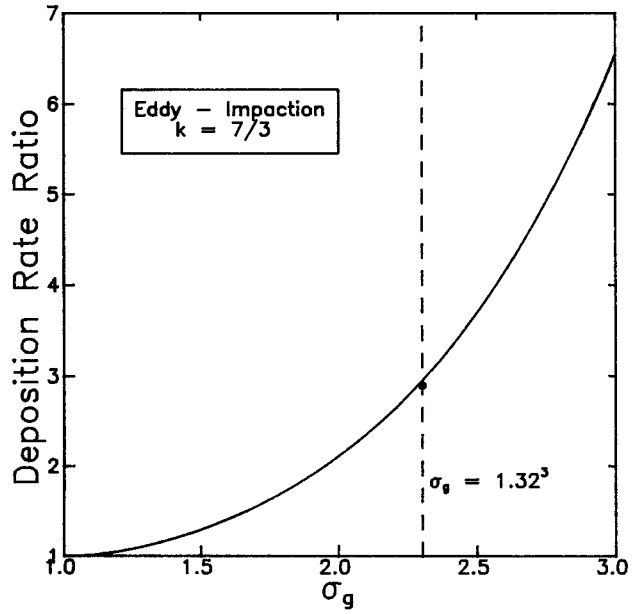

Figure 3. Deposition rate ratio, R, vs. the standard deviation of the aerosol PSD, σ_g, for eddy impaction of dense particles.

Deposition from Log-Normal Distributions When $St_m(v)$ Is a Piecewise Power-Law

In most situations of practical interest one cannot assume a single deposition mechanism: i.e., $St_m(v)$ is not a simple power law throughout the relevant range of particle sizes, especially if the particle-size distribution of the depositing aerosol is rather broad. On the other hand, quite often $St_m(v)$ is well-approximated by a piecewise power law, as in the case of turbulent deposition in duct flow systems (McCoy and Hanratty, 1977; Papavergos and Hedley, 1984). In particular, if we consider turbulent deposition in the absence of appreciable particle sedimentation effects, there is both experimental (McCoy and Hanratty, 1977) and theoretical evidence for the case of convective diffusion (e.g., Friedlander, 1977) that:

$$\frac{St_m}{\left(\frac{1}{2}C_f\right)^{1/2}} \simeq \begin{cases} 0.086\,(Sc)^{-0.701} & \text{for } t_p^+ \le t_{p,1}^+(Sc) \\ 3.25\times 10^{-4}(t_p^+)^2 & \text{for } t_{p,1}^+(Sc) \le t_p^+ \le 22.9 \\ 0.17 & \text{for } t_p^+ \ge 22.9 \end{cases} \quad (14)$$

where C_f is the nondimensional wall-friction coefficient, Sc is the particle Schmidt number ($\equiv \nu/D_p \sim v^{-1/3}$ for continuum diffusion), and t_p^+ the dimensionless particle stopping time, defined by:

$$t_p^+ \equiv \frac{u_*^2 t_p}{\nu}$$

u_* is the so-called friction velocity $(\bar{\tau}_w/\rho)^{1/2}$, and t_p the characteristic particle stopping time ($\equiv [\tilde{\rho}_p d_p^2/(18\mu)] \sim v^{2/3}$). In Eq. 14, $t_{p,1}^+(Sc)$ denotes the dimensionless particle stopping time which marks the transition from a convective-diffusion to an eddy-impaction transport mechanism, clearly a function of the particle Schmidt number (see Eq. 17; Rosner, 1988). A typical value for $t_{p,1}^+$ is about 0.2 (McCoy and Hanratty, 1977), and further let $v_{\text{crit},1}$ denote the particle size corresponding (in the prevailing environment) to this dimensionless relaxation time, e.g., the particle size at which the deposition mechanism is assumed to change abruptly from convective diffusion to eddy impaction. Similarly, let $v_{\text{crit},2}$ denote the particle size at which the particle/fluid decoupling (inertial cut-off) occurs, and define

$$r \equiv \frac{v_{\text{crit},2}}{v_{\text{crit},1}} \simeq \left(\frac{22.9}{0.2}\right)^{3/2} = 1{,}225 \quad (15)$$

where r reflects the extent of the particle-size range that deposits due to the eddy-impaction mechanism. Equation 14 can now be rewritten in terms ov v and r as follows:

$$St_m \sim \begin{cases} v_{\text{crit},1}^{0.2337}\, v^{-0.2337} & \text{for } 0 < v \le v_{\text{crit},1} \\ v_{\text{crit},1}^{-1.3333}\, v^{1.3333} & \text{for } v_{\text{crit},1} \le v \le v_{\text{crit},2} \\ r^{1.333} & \text{for } v_{\text{crit},2} \le v < \infty \end{cases} \quad (16)$$

where we required $St_m(v)$ to be a continuous function of v. The piecewise power law dependence of the dimensionless mass transfer coefficient on the particle size is clearly shown in Figure

4, where we plot $St_m/(\frac{1}{2}C_f)^{1/2}$ vs. the dimensionless particle stopping time, t_p^+. The experimental data in this figure have been compiled by McCoy and Hanratty (1977), and Ganic and Mastanaiah (1981).

In their review papers, both McCoy and Hanratty (1977), and Papavergos and Hedley (1984) imply that the dimensionless particle relaxation time at which the deposition mechanism changes from convective diffusion to eddy impaction is constant (specifically independent of particle Schmidt number) and equal to about 0.2 (cf. Eq. 14). Using their data, we estimated r (Eq. 15) to be equal to about 1,225. However, in order to obtain the general dependence of r on the particle Schmidt number, we use the fact that $St_m(v)$ is a continuous function of v. By equating the mass Stanton number that one predicts for convective diffusion at $v_{crit,1}$ to the eddy impaction $St_m(v_{crit,1})$ we find:

$$0.086[Sc(v_{crit,1})]^{-0.701} = 3.25 \times 10^{-4}[t_p^+(v_{crit,1})]^2$$

or

$$t_p^+(v_{crit,1}) = 16.27[Sc(v_{crit,1})]^{-0.35} \sim v_{crit,1}^{-0.12}$$

Using the last equation we find for r (see also Eq. 15) that

$$r = \left(\frac{22.9}{16.27[Sc(v_{crit,1})]^{-0.35}}\right)^{3/2} = 1.67[Sc(v_{crit,1})]^{-0.53} \sim v_{crit,1}^{-0.18}, \quad (17)$$

for example, the regime over which eddy impaction is important as parameterized here by r varies approximately with the inverse of the square root of the particle Schmidt number.

In order to calculate the deposition rate ratio R, it is useful to break the v space in three regimes, one for each mode of deposition, that is

$$R = \frac{\int_0^{v_{crit,1}} St_m(v)vC_1(v)\,dv}{St_m(\bar{v})\bar{v}} + \frac{\int_{v_{crit,1}}^{v_{crit,2}} St_m(v)vC_1(v)\,dv}{St_m(\bar{v})\bar{v}} + \frac{\int_{v_{crit,2}}^{\infty} St_m(v)vC_1(v)\,dv}{St_m(\bar{v})\bar{v}} \quad (18)$$

In Appendix A we show that the partial moment of any log-normal distribution can be expressed in terms of error functions as follows:

$$\int_\alpha^\beta v^q C_1(v)\,dv = \frac{1}{2}\exp\left[q\ln v_g + \frac{1}{2}q^2\ln^2\sigma_g\right] \cdot \left\{\mathrm{erf}\left[\frac{\ln\left(\frac{\beta}{v_g}\exp(-q\ln^2\sigma_g)\right)}{\sqrt{2}\ln\sigma_g}\right] - \mathrm{erf}\left[\frac{\ln\left(\frac{\alpha}{v_g}\exp(-q\ln^2\sigma_g)\right)}{\sqrt{2}\ln\sigma_g}\right]\right\} \quad (19)$$

Using Eqs. 18 and 19, and after some algebra, we can determine R for any log-normal distribution with arithmetic mean $\bar{v}$ (see Eq. 9 for the relationship between $\bar{v}$ and v_g), and standard deviation σ_g. We define here $\xi \equiv \bar{v}/v_{crit,1}$, and for brevity we also introduce the function $E(P, x)$, such that:

$$E(P, x) \equiv \mathrm{erf}\left[\frac{\ln\left(P \cdot \exp\left(-\frac{1+2x}{2}\ln^2\sigma_g\right)\right)}{\sqrt{2}\ln\sigma_g}\right] \quad (20)$$

If we denote by a, b, and c the exponents that characterize the dependence of St_m on particle volume in the convective diffusion, eddy-impaction and inertial cut-off regimes, respectively, (e.g., $a = -0.701$, $b = 1.3333$, and $c = 0$; see Eq. 18), then we find that for $v \le v_{crit,1}$ or equivalently for $\xi \le 1$

$$R = \frac{1}{2}\exp\left[\frac{a(a+1)}{2}\ln^2\sigma_g\right]\cdot\left\{E\left(\frac{1}{\xi}, a\right) + 1\right\} + \frac{1}{2}\xi^{b-a}\exp\left[\frac{b(b+1)}{2}\ln^2\sigma_g\right]\cdot\left\{E\left(\frac{r}{\xi}, b\right) - E\left(\frac{1}{\xi}, b\right)\right\} + \frac{1}{2}\xi^{c-a}r^{b-c}\exp\left[\frac{c(c+1)}{2}\ln^2\sigma_g\right]\cdot\left\{1 - E\left(\frac{r}{\xi}, c\right)\right\} \quad (21a)$$

For $v_{crit,1} \le \bar{v} \le v_{crit,2}$, or $1 \le \xi \le r$, we find

$$R = \frac{1}{2}\xi^{a-b}\exp\left[\frac{a(a+1)}{2}\cdot\ln^2\sigma_g\right]\cdot\left\{E\left(\frac{1}{\xi}, a\right) + 1\right\} + \frac{1}{2}\exp\left[\frac{b(b+1)}{2}\ln^2\sigma_g\right]\cdot\left\{E\left(\frac{r}{\xi}, b\right) - E\left(\frac{1}{\xi}, b\right)\right\} + \frac{1}{2}\xi^{c-b}r^{b-c}\exp\left[\frac{c(c+1)}{2}\ln^2\sigma_g\right]\cdot\left\{1 - E\left(\frac{r}{\xi}, c\right)\right\} \quad (21b)$$

And finally for $r \le \xi < \infty$, we find

$$R = \frac{1}{2}\xi^{a-c}r^{c-b}\exp\left[\frac{a(a+1)}{2}\ln^2\sigma_g\right]\cdot\left\{E\left(\frac{1}{\xi}, a\right) + 1\right\} + \frac{1}{2}\xi^{b-c}r^{c-b}\exp\left[\frac{b(b+1)}{2}\ln^2\sigma_g\right]\cdot\left\{E\left(\frac{r}{\xi}, b\right) - E\left(\frac{1}{\xi}, b\right)\right\} + \frac{1}{2}\exp\left[\frac{c(c+1)}{2}\ln^2\sigma_g\right]\cdot\left\{1 - E\left(\frac{r}{\xi}, c\right)\right\} \quad (21c)$$

In Figure 5, we plot deposition rate ratio, R, vs. $\xi = v/v_{crit,1}$, for different values of σ_g, and for $r = 1{,}225$ (Eq. 15). For $\xi \ll 1$, deposition occurs primarily due to convective diffusion, and indeed the deposition rates we compute here are identical to the deposition rates found earlier for the case of a single transport mechanism (see, e.g., previous two sections and Figure 1). As ξ increases and becomes closer to unity, R increases for two reasons:

- A greater fraction of the large particles and hence a greater fraction of the aerosol mass deposits due to an eddy-impaction mechanism
- At the same time the reference deposition rate, $-\dot{m}''_{p,ref}(\bar{v})$, decreases, until for ξ equal to unity R obtains its maximum value.

Note also, that the higher the standard deviation of the PSD, the earlier, with respect to ξ values, the deposition rate ratio starts increasing. As ξ increases further above unity, R

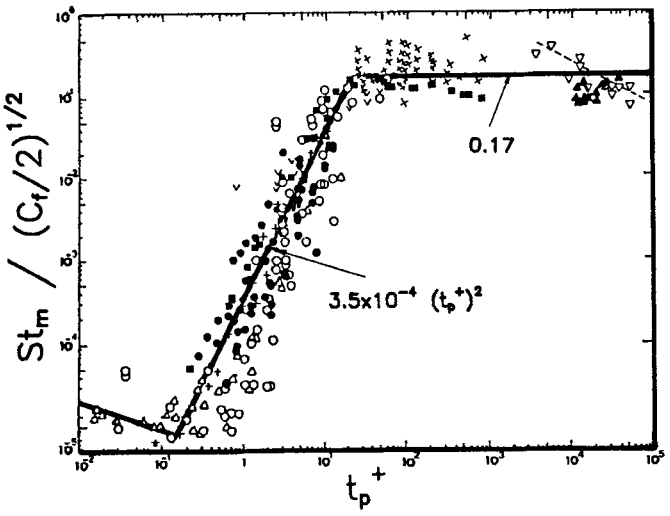

Figure 4. Literature deposition data for fully-developed duct flow in the absence of appreciable sedimentation effects.

Piecewise power law dependence of the dimensionless mass transfer coefficient on the particle stopping time.
Source: McCoy and Hanratty (1977), and Ganic and Mastanaiah (1981).

decreases towards a steady value that corresponds to deposition due to a purely eddy-impaction mechanism (compare with Figure 3). The small decrease of R, which occurs for ξ slightly larger than unity, is due primarily to an increase of the reference deposition rate in this region. Finally, as the mean volume of the distribution increases further and approaches the critical volume above which capture becomes independent of particle size (inertial cut-off), the deposition rate ratio begins to decrease, goes through a local minimum at $\bar{v} = v_{crit,2}$, or equivalently at $\xi = r$ (which we can rationalize with arguments similar to the ones we used for $\xi = 1$), and then, as expected, approaches unity. A rather interesting general implication of the local extremum exhibited by the total deposition rate ratio, $-\dot{m}_p''/-\dot{m}_{pref}''$, for particle sizes that correspond to a transition in the deposition mechanism, is that *R will not necessarily fall between the limits obtained for either of the two mechanisms acting alone.* In the present case, the deviations are quite small (for, say, convective diffusion/eddy impaction, and $\sigma_g = 1.35$, the deviation is less than 10%); but under different deposition conditions (cf. convective diffusion and inertial impaction on a cylinder in cross flow), they can become very large. In such situations, one should exercise caution when basing total mass deposition predictions exclusively on the reference deposition rate, which (by definition) is based on a single mechanism.

In Figure 6, we plot again the deposition rate ratio vs. $\xi = v/v_{crit,1}$, for $\sigma_g = 2.5$ and different values of $r = v_{crit,2}/v_{crit,1}$. As expected, the closer the two transition volumes $v_{crit,1}$ and $v_{crit,2}$ are, or equivalently for smaller r's, the importance of the eddy-impaction mechanism decreases. Note that this effect will become even more pronounced as the standard deviation, σ_g of the PSD of the depositing aerosol increases.

An examination of Figure 5, suggests that an aerosol with unimodal PSD of typical spread (σ_g of about 2.0 to 3.0) and under typical deposition conditions, say, $r = O(10^3)$, will "experience" a single or at most a combination of two transport mechanisms, that is, convective-diffusion/eddy-impaction or eddy-impaction/inertial deposition, regardless of where the mean of the particle-size distribution is located with respect to the sizes that mark the transition between the various mechanisms. On the other hand, if the PSD is bimodal or even multimodal, like, for example, in the case of supermicron particle deposition in the presence of condensible vapors (a problem of great practical interest; Rosner and Nagarajan, 1987), then all three transport mechanisms will have to be considered simultaneously.

Limiting ourselves to distributions with a single mode, we

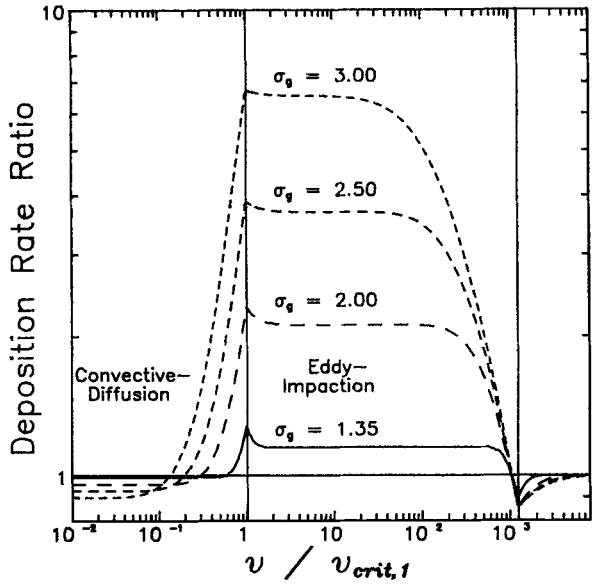

Figure 5. Deposition rate ratio *R* vs. dimensionless mean size of particle size distribution for various values of PSD standard deviation.

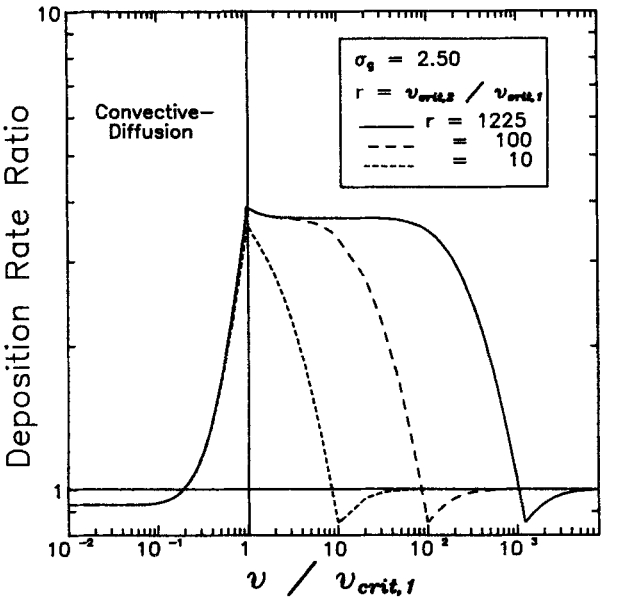

Figure 6. Effect of the extent of the eddy-impaction regime, as determined by *r*, on the deposition rate ratio *R* for a PSD with $\sigma_g = 2.5$.

present in Figure 7 curves of constant deposition rate ratio R on a σ_g vs. $\bar{v}/v_{crit}$ plot for the case of deposition due to convective-diffusion and eddy-impaction. This figure is a cross plot of the left half of Figure 5 and can be readily used to determine the deposition rate ratio as a function of the location of the PSD mean with respect to v_{crit} as determined by the local conditions and the PSD standard deviation. Thus, for $(\bar{v}/v_{crit}, \sigma_g)$ pairs that lie in the shaded region (region II), both mechanisms have to be considered. In this case, a first estimate of the deposition rate ratio can be obtained from the given iso-R curves. If, on the other hand, the pairs lie in regions I or III, then the deposition is determined primarily by a single mechanism, and so Eq. 13 can be used with an expected accuracy of ±3%. A similar plot for eddy impaction/inertial deposition is given in Figure 8. In region I Eq. 13 may again be used, but in region III the deposition rate ratio is equal to unity.

Generalizations

Finite-analytic procedure for calculating total deposition rates

In this section, we outline a "finite-analytic" method that allows us to compute total mass deposition rates in the general case where $St_m\{v\}$ is an arbitrary function of particle volume. The basic idea is simple indeed: since log (St_m) vs. log $\{v\}$ can be approximated to any desired degree of accuracy by a series of straight line segments, St_m can be always reduced to a piecewise power law. But, recall that for this case we already have an analytic solution (cf. previous two sections). In Appendix B, we give an expression for

$$R = \frac{-\dot{m}''_{p,tot}}{-\dot{m}''_p\{\bar{v}\}} = \frac{\sum_{i=1}^{N} \int_{v_{i-1}}^{v_i} St_{m,i} v C_1\{v\}\, dv}{St_{m,k}\{\bar{v}\}\bar{v}} \qquad (21)$$

for the case of St_m consisting of say N discrete power-law segments, and the *arithmetic mean volume* of the aerosol population $\bar{v}$ lying in the kth interval In Eq. 21, we assume that $v_1 = 0$ and $v_N = \infty$.

Clearly in implementing this method, one should approximate St_m by a *larger* number of *shorter* straight line segments wherever the curvature is higher. In order to test whether in any given particle volume regime, (v_{k-1}, v_k), the power-law approximation is adequate we propose the following simple criterion (Rosner, 1989). By expanding ln $St_m(\bar{v})$ vs. ln v in a Taylor series around $\bar{v}$ and inserting into Eq. 21, we find that this approximation is acceptable provided:

$$\frac{\sum_{i=1}^{N} \int_{v_{i-1}}^{v_i} \frac{1}{2!} \left(\frac{\partial^2 \ln St_m}{\partial (\ln v)^2}\right)_{v=\bar{v}} \left(\ln \frac{v}{\bar{v}}\right)^2 v C_1\{v\}\, dv}{R \cdot \left[(\ln St_m)_{v=\bar{v}} + \left(\frac{\partial \ln St_m}{\partial \ln v}\right)_{v=\bar{v}} \cdot \left(\ln \frac{v}{\bar{v}}\right)\right] \cdot \bar{v}} \ll 1 \qquad (22)$$

This criterion can be readily introduced into a general-purpose code, so that the number and location of the straight line segments that are needed to approximate a given capture efficiency curve is optimal. In the present illustrative calculations (cf. Figures 9 and 10), however, we simply increased the number of Δ (ln v) segments until the computed R values acceptably converged.

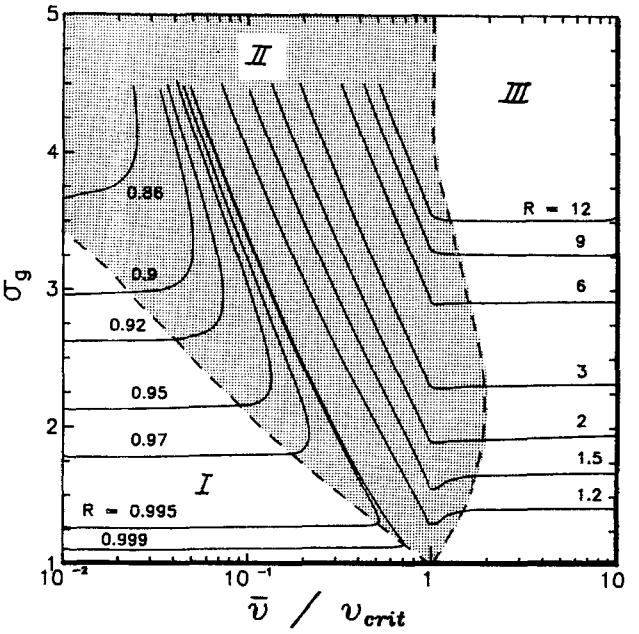

Figure 7. Constant deposition rate ratio R on σ_g vs. (log) $\bar{v}/v_{crit}$ plot for the case of deposition due to convective diffusion and eddy impaction.

In regions I and III, Eq. 13 is valid, and it is only in the shaded regime where both mechanisms must be considered simultaneously.

Convective diffusion and inertial impaction on a cylinder in cross flow

We will demonstrate the application of our method for the case of convective diffusion and inertial impaction on a cylinder in cross flow, perhaps the most important example from an engineering point of view. We will assume that the Reynolds number, Re, based on cylinder diameter, d_w, is large ($Re^{1/2} \gg 1$) and that the interception parameter, d_p/d_w, is small (at least for the particle sizes that deposit due primarily to Brownian diffusion) so that we can neglect deposition due to interception. For this simplified case, it is well known that the convective-diffusion capture efficiency, η_{cap}, defined as the fraction of the particles collected from the fluid volume swept by the cylinder, is given by (see, e.g., the Nusselt number correlations in Eckert and Drake, 1981; Perry and Chilton, 1973):

$$\eta_{cap} \equiv 2 \cdot \left(\frac{\overline{Nu}_m}{Re \cdot Sc}\right) \simeq 0.054\, Re^{-0.195} Sc^{-2/3} \qquad (23)$$

Note that, in this regime, the particle capture fraction depends on the collector-based Reynolds number and the particle Schmidt number.

In the case of "pure" inertial deposition, the capture efficiency of the cylinder depends on the particle Stokes number, Stk and, for non-Stokesian particles (because the velocity of the flow field is high and/or because the particles are large) it will also depend on a Reynolds number, Re_p, based on particle diameter and the free-stream velocity. For a potential flow field approximation to the carrier fluid motion around the collector, the collection efficiency has been calculated numerically (Brun et al., 1955) and has been also correlated in terms of an effective

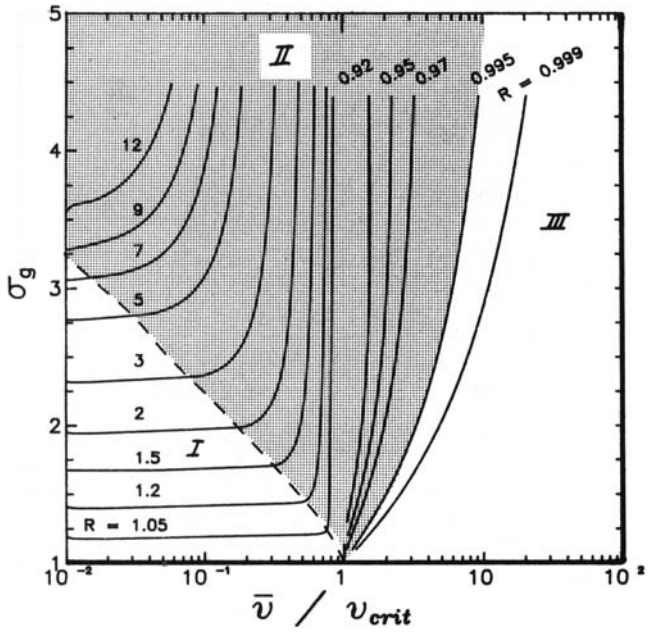

Figure 8. Constant deposition rate ratio R on a σ_g vs. (log) $\bar{v}/v_{crit}$ plot for the case of capture due to eddy impaction and inertial deposition.

In region I, Eq. 13 is valid, in the shaded area both mechanisms must be considered; in region III, the deposition rate ratio can be taken equal to unity.

Stokes number (Israel and Rosner, 1983) which accounts for the above-mentioned parameters. For these reasons Israel and Rosner (1983) introduced a generalized Stokes number:

$$Stk_{eff} = \Psi(Re_p) \cdot Stk \tag{24}$$

where for our purposes Stk is the conventionally-defined Stokes

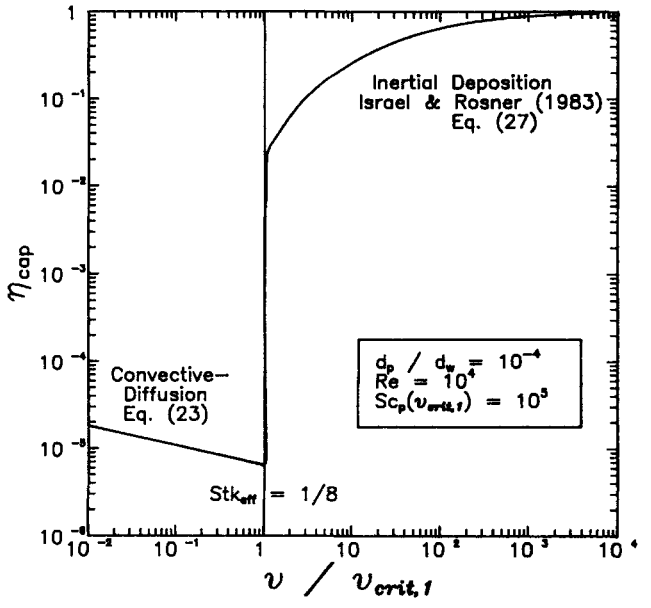

Figure 9. Typical behavior of the efficiency curve for particle capture on a circular cylinder in cross-flow in the high Reynolds number limit ($Re^{1/2} \gg 1$).

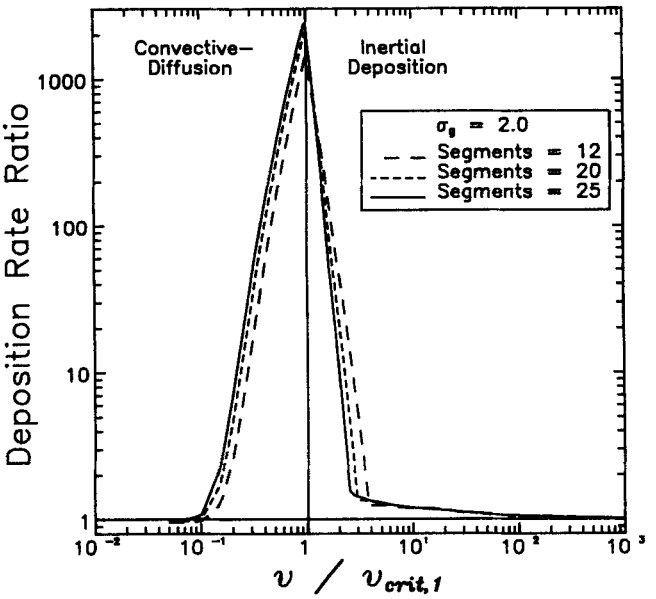

Figure 10. Convergence of the deposition rate ratio R as the number of power-law segments (used to approximate the capture efficiency curve of Figure 8) increases.

number $[=\tilde{\rho}_p d_p^2 U/(18\mu)]$ and $\Psi(Re_p)$ a correction factor to account for non-Stokesian behavior, i.e.:

$$\Psi(Re_p) = \frac{24}{Re_p} \cdot \int_0^{Re_p} \frac{dRe'}{C_D(Re')Re'} \tag{25}$$

Integrating Eq. 25 for a quasisteady drag coefficient, C_D of the commonly used approximate form

$$C_D(Re) = \frac{24}{Re}(1 + 0.158Re^{2/3})$$

one readily finds

$$\Psi(Re_p) \simeq \frac{3}{0.0628Re_p} \cdot [(0.0628Re_p)^{1/3} - \tan^{-1}\{(0.0628Re_p)^{1/3}\}] \tag{26}$$

For a circular cylinder collection geometry and $Stk_{eff} > 0.14$, Israel and Rosner (1983) recommend the following correlation for the capture fraction (if each impacting particle "sticks"):

$$\eta_{cap}(Stk_{eff}) \simeq \left[1 + 1.25\left(Stk_{eff} - \frac{1}{8}\right)^{-1} - 1.4 \times 10^{-2} \cdot \left(Stk_{eff} - \frac{1}{8}\right)^{-2} + 0.058 \times 10^{-4}\left(Stk_{eff} - \frac{1}{8}\right)^{-3}\right]^{-1} \tag{27}$$

although equally acceptable alternatives are given by Wessel and Righi (1988), and Wang (1986).

At this point, we are not aware of any correlation for $\eta_{cap}(Stk_{eff})$ in the near-critical range of Stk_{eff} (from 0.125 to 0.14),

and so for that range we simply take:

$$\eta_{cap} \simeq A \cdot \left(Stk_{eff} - \frac{1}{8}\right)^d \tag{28}$$

[In the spirit of earlier calculations of the critical Stokes number (Friedlander, 1977), such a near-Stk_{crit} relation can be derived by using a second-order expansion of the flow field in the vicinity of the forward stagnation point.] Equation 28 does exhibit the proper limiting behavior as Stk_{eff} approaches Stk_{crit}, but other than that is not based on any physical grounds. By matching Eq. 27 to Eq. 24 for $Stk_{eff} = 0.14$ and further requiring the first derivative of $\eta_{cap}\{v\}$ with respect to v to be also continuous, we estimate the two constants appearing in Eq. 28:

$$\eta_{cap} \simeq 0.043 \left(Stk_{eff} - \frac{1}{8}\right)^{0.11} \tag{29}$$

In Figure 9, we give a typical capture efficiency curve that encompasses both the convective diffusion and inertial deposition regimes. Note that, since in the convective-diffusion regime η_{cap} is already a power law, we can analytically integrate this entire size range ([0, 1] in dimensionless volume units) in one "giant" step, thus saving computational time. [If we neglect the effect of Kn_p, i.e., within the confines of continuum ($Kn_p \ll 1$) diffusion.] In Figure 10, we show the dependence of the deposition rate R on $\bar{v}/v_{crit,1}$ for a log-normal mainstream particle-size distribution that has $\sigma_g = 2.0$ and that deposits according to η_{cap} as depicted in Figure 11. Note that if we "fit" the inertial deposition part of the (log) η_{cap} vs. log $(v/\bar{v})$ curve with about 20 linear segments R converges. Finally, in Figure 11, we show the dependence of the total mass deposition rate ratio on the dimensionless mean size of the aerosol population for different values of the standard deviation of the PSD.

From Figures 10 and 11, it is clear that, in the case of deposition on a cylinder in cross flow, the total mass deposition rate ratio is a very sensitive function of the relative location of the mean particle size, $\bar{v}$, with respect to the particle size at which transition occurs from deposition due to convective diffusion to an inertial mechanism. This is another example where one should avoid basing deposition calculations on a single regime, since in this case the total deposition rate can be severely underpredicted. From a mathematical point of view, R almost diverges in the neighborhood of $\bar{v}/v_{crit} \simeq 1$, because in this regime there is a great difference of order $O(10^3)$ between the magnitude of the actual total mass deposition rate and the reference deposition rate.

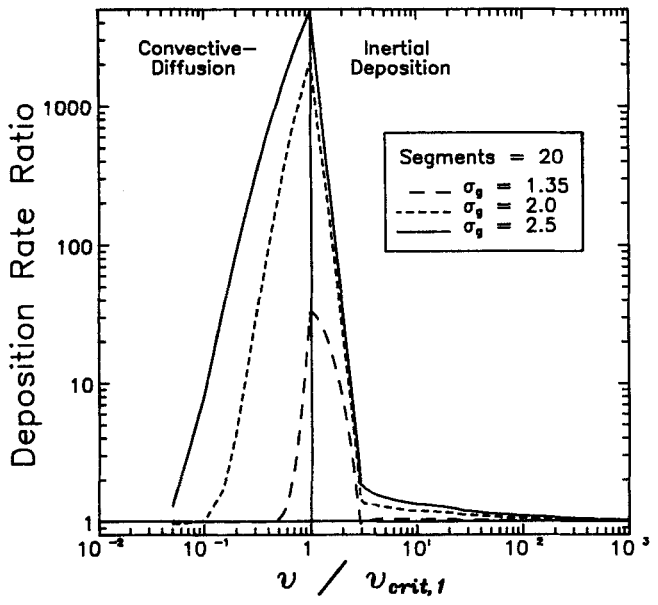

Figure 11. Dependence of the total mass deposition rate ratio on the dimensionless average size of aerosol population for different values of the PSD standard deviation.

Variance of non-log-normal single-mode distributions

In this paper we deliberately cast our results in terms of the particle arithmetic mean size (volume), $\bar{v}$, and the standard deviation, σ_g, of the aerosol PSD. We decided to use the average particle size of the population, rather than the distribution median, v_g, because the former has also a simple physical significance, despite the fact that, if we had used v_g, some of our analytical expressions would have been simplified. By the same token, we have here used σ_g to quantify the spread of the (log-normal) distribution, a natural choice from a mathematical point of view, while we could also have used the square root of the dimensionless variance of the PSD, here denoted simply by σ and defined as

$$\sigma \equiv \left[\frac{1}{\bar{v}} \cdot \int_0^\infty (\bar{v} - v)^2 C_1\{v\}\, dv\right]^{1/2} = [\exp\{\ln^2\sigma_g\} - 1]^{1/2} \tag{30}$$

Since not all single-mode PSD's are "log-normal," we conjecture that, if our present results were recast in terms of the square root of the variance σ, then they would (approximately) apply to a wide variety of single-mode distributions.

Conclusions

For commonly encountered engineering applications, in which total mass deposition rates are required from fluid streams containing suspended particles distributed near "log-normally," we have developed and presented simple results for piecewise-power-law mass transfer coefficients (e.g., turbulent convective diffusion and eddy impaction) (including an inertial decoupling "cut-off"). Thus, we have shown that, whenever we may assume a simple power-law dependence of $St_m\{v\}$ on the size of the depositing particles, the total mass deposition rate ratio, R, is given analytically by a very simple expression that involves only the exponent that describes the dependence of the mass Stanton number on particle volume and the spread of the aerosol PSD, σ_g (cf. Eq. 13). We further obtained analytical expressions (in terms of error functions) for R in the case of piecewise-power-law mass transfer coefficients, St_m, (Eq. 21 and Appendix B) which can be readily used in computations and have also provided graphs (Figures 7 and 8) from which one can directly obtain the local deposition rate ratio for the commonly-encountered case of deposition due to a combination of convective-diffusion/eddy-impaction or eddy-impaction/inertial mechanism.

These results/plots, which generalize the recent conclusions of Rosner (1989) for power-law capture from coagulation-aged (self-preserving shape) aerosols, reduce the general problem of

computing actual deposition rates to the straightforward one of first calculating the (reference) deposition rate if all particles in the population had the same (average) volume and then correcting this result by a ratio R calculated here for several commonly-encountered mechanistic combinations over a range of aerosol PSD "spread" parameters. Apart from their direct engineering utility and conceptual value, our viewpoint and procedures are shown to open the way to computationally-efficient finite-analytic methods for computing total mass deposition rates from aerosol population distributions of *arbitrary* shape, captured in accord with an efficiency function of *arbitrary* shape. [Indeed, this strategy could clearly be adopted to compute many other properties of aerosol populations which require the integral of a product of the particle-size distribution function and some other particle-size-dependent quantity, e.g., light scattering efficiency (Buckius and Hwang, 1980).]

It would be prudent to recall the most important assumption which underlies our present methods and predictions: viz., *each particle size class does not influence the deposition rate of other size classes.* In practice, we know that this assumption would have to be relaxed whenever:

- The diffusional capture of small particles influences the inertial capture (via sticking probability) of larger particles (see, e.g., Rosner and Nagarajan, 1987)
- Appreciable particle-particle coagulation occurs in the immediate vicinity of the collector (see, e.g., Park and Rosner, 1988a; Biswas, 1988)
- A portion of the preexisting aerosol population coupled with the host fluid flow to modify the transfer coefficient of the smaller particles (see, e.g., Park and Rosner, 1988b, 1989)
- The depositing particles scavenge an appreciable mass of coexisting vapor within the thermal boundary layer adjacent to the collector (see, e.g., Castillo and Rosner, 1988)
- Appreciable particle production (from a supersaturated vapor) occurs within the thermal boundary layer adjacent to the collector (see, e.g., Castillo and Rosner, 1989; Liang et al., 1989).

However, even in most of these more complex (coupled) cases, it will still be useful and instructive to compare actual rates to those expected based on the simple procedure outlined in this paper.

Finally, it should be recognized that in many current and future applications, in addition to predicting the total deposit mass, it will be necessary to have a quantitative understanding of the *deposit microstructure* and, of course, microstructure-sensitive deposit properties (see, e.g., Tassopoulos et al., 1989). This is clearly a more ambitious goal of deposition rate theory, but one which can no longer be postponed.

Acknowledgment

It is a pleasure to acknowledge the financial support of DOE-PETC via Grant No. DE-FG22-86PC90756 and the U.S. AFOSR via Grant No. AFOSR 84-0034, 89-0223, as well as the related support of the Yale HTCRE Laboratory by our current Industrial Affiliates: Shell Foundation, Lycoming-Textron, and SCM-Chemicals. In this research, the authors have benefited from helpful discussions with Professors J. Fernandez de la Mora and J. O'Brien, Dr. D. W. Mackowski, as well as A. G. Konstandopoulos.

Notation

b = exponent characterizing dependence of St_m on particle volume v
C_f = nondimensional wall-friction coefficient; $=\bar{\tau}_w/(\frac{1}{2}\rho U^2)$
C_D = quasisteady particle drag coefficient
$C_i\{v\}$ = normalized log-normal distribution function, Eq. 8
d_p = particle diameter
d_w = circular cylinder (target) diameter
D_p = particle Brownian diffusion coefficient
$E\{P, x\}$ = function, Eq. 20
k = "order" of PSD moment
Kn_p = particle Knudsen number, l/d_p
l = gas-mean-free path
$-\dot{m}''_p$ = total mass deposition rate, Eq. 4
$-\dot{m}''_{p,\text{ref}}$ = reference mass deposition rate, Eq. 5
$n\{v\}$ = particle number density function
N_p = particle number density, Eq. 1
P = dummy variable, Eq. 20
Pe = Peclet number for particle diffusion
q = "order" of partial moment of log-normal distribution, Eq. 19
r = parameter reflecting extent of the particle size range over which eddy impaction is the predominant deposition mechanism
R = deposition rate ratio, Eq. 6
Re = Reynolds number based on cylinder diameter
Re_p = Reynolds number based on particle diameter
Sc = particle Schmidt number
St_m = dimensionless mass transfer coefficient
Stk = particle Stokes number
Stk_{eff} = effective particle Stokes number, Eq. 24
t_p = characteristic particle stopping time
t_p^+ = dimensionless particle stopping time, $u_*^2 t_p/\nu$
$t_{p,1}^+$ = dimensionless particle stopping time marking transition from convective-diffusion to eddy-impaction deposition
u_* = friction velocity; $(C_f/2)^{1/2}U$
U = gas-free-stream velocity
v = particle size (volume)
$\bar{v}$ = mean particle volume; ϕ_p/N_p
v_{crit} = particle size marking a transition in deposition mechanism
$v_{\text{crit},1}$ = particle size marking transition from a convective-diffusion to eddy-impaction deposition mechanism; Figure 4
$v_{\text{crit},2}$ = particle size marking transition from eddy-impaction to size-insensitive deposition; Figure 4
v_g = median volume of log-normal distribution
v_i = critical particle size marking beginning of the $(i+1)$ deposition regime
v_k = median volume of a particular log-normal distribution function, Eq. 11
v_* = dimensionless particle size $(=v/v_g)$
x = dummy variable, Eq. 20

Greek letters

α = lower limit of partial moment of log-normal distribution, Eq. 19
β = upper limit of partial moment of log-normal distribution, Eq. 19
η_{cap} = capture fraction
μ = gas dynamic viscosity
ν = gas momentum diffusivity (kinematic viscosity)
ξ = dimensionless mean particle size $(=\bar{v}/v_{\text{crit}})$
ρ = gas density
$\tilde{\rho}_p$ = intrinsic particle density
σ^2 = dimensionless variance of log-normal distribution, Eq. 30
σ_g = geometric standard deviation of log-normal distribution
ϕ_p = particle volume fraction, Eq. 1
Ψ = self-preserving distribution function
Ψ = correction factor accounting for non-Stokesian drag behavior of particles, Eqs. 24, 25

Literature Cited

Ali, S. I., and R. L. Zollars, "Generation of Self-Preserving Particle Size Distributions during Shear Coagulation," *J. Coll. Interf. Sci.*, **126**, 377 (1988).

Aitchison, J., and J. A. C. Brown, *The Log-Normal Distribution*, Cambridge University Press (1969).

Biswas, P., "Differential Impaction of Aerosols," *J. Aerosol Sci.*, **19**, 603 (1988).
Brun, R. J., W. Lewis, P. J. Perkins, and J. S. Serafini, "Impingement of Cloud Droplets on a Cylinder and Procedure for Measuring Liquid-Water Content and Droplet Sizes in Supercooled Clouds by Rotating Multicylinder Method," NACA Rep. 1215 (1955).
Buckius, R. O., and D. C. Hwang, "Radiation Properties for Polydispersions: Application to Coal," *ASME J. Heat Transfer*, **102**, 99 (1980).
Castillo, J. L., and D. E. Rosner, "Nonequilibrium Theory of Surface Deposition from Particle-Laden, Dilute Condensible Vapor-Containing Stream, Allowing for Particle Thermophoresis and Vapor Scavenging within the Laminar Boundary Layer," *Int. J. Multiphase Flow*, **14**(1), 99 (1988).
Castillo, J. L., and D. E. Rosner, "Theory of Surface Deposition from a Binary Dilute Vapor-Containing Stream, Allowing for Equilibrium Condensation within the Laminar Boundary Layer," *Int. J. Multiphase Flow*, **15**(1), 97 (1989).
Eckert, E. R. G., and R. M. Drake, Jr., *Heat and Mass Transfer*, R. E. Krieger, FL (1981).
Fernandez de la Mora, J., and D. E. Rosner, "Effects of Inertia on the Diffusional Deposition of Small Particles to Spheres and Cylinders at Low Reynolds Numbers," *J. Fluid Mech.*, **125**, 379 (1982).
Flagan, R., and S. K. Friedlander, *Recent Developments in Aerosol Science*, J. Davis, ed., Wiley, New York, 25 (1978).
Friedlander, S. K., *Smoke, Dust and Haze-Fundamentals of Aerosol Behavior*, Wiley, New York (1977).
Friedlander, S. K., and C. S. Wang, "The Self-Preserving Particle Size Distribution for Coagulation by Brownian Motion," *J. Coll. Interf. Sci.*, **22**, 126 (1966).
Fuchs, N. A., *Mechanics of Aerosols*, Pergamon, New York (1964).
Ganic, E. N., and K. Mastanaiah, "Investigation of Droplet Deposition from a Turbulent Gas Stream," *Int. J. Multiphase Flow*, **7**, 401 (1981).
Garber, E., S. G. Brush, and C. W. F. Everitt, *Maxwell on Molecules and Gases*, MIT Press, Cambridge, MA (1986).
Israel, R., and D. E. Rosner, "Use of a Generalized Stokes Number to Determine the Aerodynamic Capture Efficiency of Non-Stokesian Particles from a Compressible Gas Flow," *Aerosol Sci. Tech.*, **2**, 45 (1983).
Lai, F. S., S. K. Friedlander, J. Pich, and G. M. Hidy, "The Self-Preserving Particle Size Distribution for Brownian Coagulation in the Free-Molecule Regime," *J. Coll. Interf. Sci.*, **39**(2), 395 (1972).
Lee, K. W., "Change of Particle Size Distribution during Brownian Coagulation," *J. Coll. Interf. Sci.*, **92**, 315 (1983).
Lee, K. W., H. Chen, and J. A. Gieseke, "Log-Normal Preserving Size Distribution for Brownian Coagulation in the Free-Molecule Regime," *Aerosol Sci. Tech.*, **3**, 53 (1984).
Liang, B., A. Gomez, J. L. Castillo, and D. E. Rosner, "Experimental Studies of Nucleation Phenomena within Thermal Boundary Layers—Influence on Chemical Vapor Deposition Rate Processes," *Chem. Eng. Comm.*, in press (1989).
McCoy, D. D., and T. J. Hanratty, "Rate of Deposition of Droplets in Annular Two-Phase Flow," *Int. J. Multiphase Flow*, **3**, 319 (1977).
Meakin, P., "Diffusion-Controlled Cluster Formation in 2-6-Dimensional Space," *Phys. Rev. A*, **27**, 1495 (1983).
Mountain, R. D., G. W. Mulholland, and H. Baum, "Simulation of Aerosol Agglomeration in Free-Molecular and Continuum Flow Regimes," *J. Coll. Interf. Sci.*, **114**(1), 67 (1986).
Papavergos, P. G., and A. B. Hedley, "Particle Deposition Behavior from Turbulent Flows," *Chem. Eng. Res. Des.*, **62**, 275 (1984).
Park, H. M., and D. E. Rosner, "Boundary Layer Coagulation Effects on the Size Distribution of Thermophoretically Deposited Particles," *Chem. Engrg. Sci.*, in press (1988).
———, "Combined Inertial and Thermophoretic Effects on Particle Deposition Rates in Highly Loaded Dusty Gas Systems," *Chem. Eng. Sci.*, in press (1989).
Perry, R. H., and C. H. Chilton, *Chemical Engineers' Handbook*, McGraw Hill, New York (1971).
Raabe, O. G., "Particle Size Analysis Utilizing Grouped Data and the Log-Normal Distribution," *J. Aerosol Sci.*, **2**, 289 (1971).
Rosner, D. E., "Total Mass Deposition Rates from Polydispersed Aerosols," *AIChE J.*, **35**, 164 (Jan., 1989).
———, *Transport Processes in Chemically Reacting Flow Systems*, 2nd Printing, Butterworth, Stoneham, MA (1988).
Rosner, D. E., and H. M. Park, "Thermophoretically Augmented Mass-, Momentum-and Energy-Transfer Rates in High Particle Mass-Loaded Laminar Forced Convection Systems," *Chem. Eng. Sci.*, **43**(10), 2689 (1988).
Rosner, D. E., and R. Nagarajan, "Toward a Mechanistic Theory of Net Deposit Growth from Ash-Laden Flowing Combustion Gases: Self-Regulated Sticking of Impacting Particles and Deposit Erosion in the Presence of Vapor Glue," *AIChE Symp. Ser.*, **83**(257), R. W. Lyczkowski, ed., 289 (1987).
Tassopoulos, M., J. A. O'Brien, and D. E. Rosner, "Simulation of Microstructure/Mechanism Relationships in Deposition," *AIChE J.*, **35**, 967 (June, 1989).
Wang, C. S., and S. K. Friedlander, "The Self-Preserving Particle Size Distribution for Coagulation by Brownian Motion," *J. Coll. Interf. Sci.*, **24**, 170 (1967).
Wang, H. C., "Theoretical Adhesion Efficiency for Particles Impacting a Cylinder at High Reynolds Number," *J. Aerosol Sci.*, **17**, 827 (1986).
Wessel, R. A., and J. Righi, "Generalized Correlations for Inertial Impaction of Particles on a Circular Cylinder," *Aerosol Sci. Tech.*, **9**, 29 (1988).

Appendix A: Partial Moments of Log-Normal Distribution

The log-normal particle-size distribution is given by:

$$C_1(v) = \frac{1}{v \ln \sigma_g \sqrt{2\pi}} \exp\left[-\frac{\ln^2 (v/v_g)}{2 \ln^2 \sigma_g}\right] \qquad (0 < v < \infty) \quad \text{(A1)}$$

The partial moment, μ_q, of order q, in the range say α to β, is defined here by:

$$\mu_q \equiv \int_\alpha^\beta v^q C_1(v)\, dv \quad \text{(A2)}$$

Note further that for any log-normal distribution (Raabe, 1972)

$$v^q C_1(v) = \exp\left[q \ln v_g + \frac{q^2}{2} \ln^2 \sigma_g\right] \cdot \left\{\frac{1}{v \ln \sigma_g \sqrt{2\pi}} \exp\left[-\frac{\ln^2 (v/v_q)}{2 \ln^2 \sigma_g}\right]\right\} \quad \text{(A3)}$$

where

$$\ln v_q = \ln v_g + q \ln^2 \sigma_g \quad \text{(A4)}$$

From Eqs. A1, A2 and A3, we obtain for the partial moment

$$\mu_k = \exp\left[q \ln v_g + \frac{q^2}{2} \ln^2 \sigma_g\right] \cdot \int_\alpha^\beta \frac{1}{v \ln \sigma_g \sqrt{2\pi}} \exp\left[-\frac{\ln^2 (v/v_q)}{2 \ln^2 \sigma_g}\right] dv \quad \text{(A5)}$$

with the distribution in the definite integral of Eq. A5 another log-normal. Noting also that in general the log-normal is defined as a distribution of sizes whose logarithms are normally distributed, it becomes apparent that the required definite integral can be expressed in terms of the well-known error function. Specifi-

cally, we have

$$\int_{\alpha}^{\beta} \frac{1}{v \ln \sigma_g \sqrt{2\pi}} \exp\left[-\frac{\ln^2(v/v_g)}{2 \ln^2 \sigma_g}\right] dv = \int_{\ln(\alpha/v_q)/\ln\sigma_g}^{\ln(\beta/v_q)/\ln\sigma_g} \frac{1}{\sqrt{2\pi}} \exp\left[-\frac{1}{2}\left(\frac{\ln(v/v_q)}{\ln\sigma_g}\right)^2\right] d\left(\frac{\ln(v/v_q)}{\ln\sigma_g}\right)^2 = \frac{1}{2} \cdot \int_{\ln(\alpha/v_q)/\sqrt{2}\ln\sigma_g}^{\ln(\beta/v_q)/\sqrt{2}\ln\sigma_g} \frac{2}{\sqrt{\pi}} \exp - t^2 \, dt \quad \text{(A6)}$$

Combining now Eqs. A4 and A6, while substituting for v_q from Eq. A4, we obtain for the partial moment of order q:

$$\mu_q \int_{\alpha}^{\beta} v^q C_1(v)\, dv = \frac{1}{2} \exp\left[q \ln v_g + \frac{1}{2} q^2 \ln^2 \sigma_g\right] \cdot \left\{ \operatorname{erf}\left[\frac{\ln\left(\frac{\beta}{v_g} \exp(-q \ln^2 \sigma_g)\right)}{\sqrt{2} \ln \sigma_g}\right] - \operatorname{erf}\left[\frac{\ln\left(\frac{\alpha}{v_g} \exp(-q \ln^2 \sigma_g)\right)}{\sqrt{2} \ln \sigma_g}\right]\right\} \quad \text{(A7)}$$

that is, Eq. 19.

Appendix B: Analytic Expression for Total Mass Deposition Rate Ratio When $St_m(v)$ Is a Piecewise Power-Law

Suppose that the mass Stanton number, $St_m(v)$, consists of N discrete power-law segments, and that the arithmetic mean of the aerosol particle-size distribution, $\bar{v}$, lies in the kth (power-law) segment. In this case, the total mass deposition rate ratio, R, is defined here by:

$$R = \frac{-\dot{m}''_{p,\text{tot}}}{-\dot{m}''_p(\bar{v})} = \frac{\sum_{i=1}^{N} \int_{v_{i-1}}^{v_i} St_{m,i} v C_1(v)\, dv}{St_{m,k}(\bar{v})\bar{v}} \quad \text{(B1)}$$

where $St_{m,i}$ denotes the Stanton mass number in the ith interval. Here we also take $v_0 = 0$ and $v_N = \infty$. If $v_{\text{crit},i}$ is the particle size (volume) that marks the transition from the ith to the $i + 1$ deposition mechanism, let

$$r_i = \frac{v_{\text{crit},i}}{v_{\text{crit},1}} \quad \text{for} \quad i = 2, N - 1 \quad \text{(B2)}$$

Since $St_m(v)$ is a continuous function of the particle size, v, it is straightforward to show that the Stanton number in the ith interval is given by

$$St_{m,i} \sim \left(\prod_{j=1}^{i-2} r_j^{b_{j+1} - b_{j+2}}\right) \cdot \xi^{b_i} \quad \text{(B3)}$$

where ξ is the dimensionless mean particle size, $\xi = \bar{v}/v_{\text{crit},1}$.

If we substitute now into Eq. B1 and use the expression for the partial moment of a log-normal distribution (Appendix A), after some algebraic manipulation one finds that

$$R = \frac{1}{2} \sum_{i=1}^{N} \frac{St_{m,i}}{St_{m,k}} \cdot \exp\left[\frac{b_i(b_i + 1)}{2} \ln^2 \sigma_g\right] \cdot \left\{E\left(\frac{r_{i-1}}{\xi}, b_i\right) - E\left(\frac{r_{i-2}}{\xi}, b_i\right)\right\} \quad \text{(B4)}$$

where E is a function introduced here for brevity, defined by Eq. 20.

Manuscript received Feb. 28, 1989, and revision received June 20, 1989.